Temporal Evolution of Drop Spectra to Collisional Equilibrium in Steady and Pulsating Rain

R. LIST, N. R. DONALDSON* AND R. E. STEWART**

Department of Physics, University of Toronto, Toronto, Ontario, Canada M5S 1A7

(Manuscript received 10 October 1985, in final form 22 August 1986)

ABSTRACT

The evolution of raindrop spectra by collisional breakup is examined analytically and modelled in box and 1-dimensional shaft models, using the parameterization of Low and List. The significant analytical result shows that equilibrium drop size distributions occur in families that are multiples of one another:

$$f(D,R) = R\psi(D)$$

where D is the drop diameter, R is the rainfall rate, $f(D, R)$ the number density distribution in terms of D and R and ψ is a shape function.

For the Low–List breakup scheme the shapes are trimodal, with peaks in the number distributions at diameters of 264, 790, and 1760 μm. Similar structures were found by Valdez and Young, and Brown for box models. These peaks are expected to exist wherever spectra approach equilibrium, independently of the rainfall rate. In this paper the development of these peaks from non-equilibrium spectra is examined, together with the effect of periodically varying rainfall rates.

In box and one-dimensional shaft models, nonequilibrium spectra quickly develop features similar to those at equilibrium, but times and/or heights to reach true equilibrium are in excess of 30 minutes or 3 km for all but the very heaviest rainfall rates. The peaks, however, should be identifiable in a matter of minutes, thus encouraging field verification under favorable conditions. In the absence of evaporation, spectral evolution below a cloud is dominated by the large drops, which produce the accompanying small drops by breakup.

Evaporation, while basically affecting the smallest drops, is quickly spread over the whole spectrum by the collision process and reduces the total liquid water content. The drop spectrum shape however, remains unchanged.

1. Introduction

The understanding of the formation of rain has progressed through many stages, each adding a new physical process or insight. Nineteenth century experiments showed and quantified how water condenses on cloud condensation nuclei suspended in the air, but Reynolds (1877) showed that this process is too slow to produce rain-sized drops in the times typically seen in clouds. According to Middleton (1966) the solution to this dilemma had been proposed by E. Barlow in 1715, but was only widely championed in the late 19th century. The differential fall velocities of droplets of different sizes result in collisions and coalescence. Wegener (1911) and Bergeron (1935) proposed that rain could also be quickly produced by the melting of ice formed on ice nuclei. In the presence of supercooled droplets, ice grows quickly at the expense of the water due to the lower equilibrium vapor pressure of ice. This fast process was not sufficient to explain all precipitation since aviators in the 1940s noted the occurrence of rain in clouds that were entirely below the freezing level. Langmuir (1948) proposed that the breakup of drops by aerodynamic forces could produce additional drops to act as new collectors of cloud droplets. This "chain reaction" theory provided both an upper limit on drop growth and a fast multiplication of drops. Many numerical modellers (e.g., Hall, 1981) have invoked aerodynamic breakup, using simple parameterizations, such as that due to Danielsen et al. (1972), as an upper boundary condition on the drop size coordinate. It has been found, however, (Pruppacher and Klett, 1978), that drops do not necessarily breakup spontaneously until they have diameters in excess of 6 mm. Magarvey and Geldart (1962) showed that collisions between drops could result in breakup and not just coalescence.

The process of collisional breakup has been fairly extensively studied in recent years, but its incorporation in numerical models in addition to coalescence has lagged due to the much greater computational effort required. Early systematic laboratory experiments on collisional breakup were conducted by List et al. (1970), Brazier-Smith et al. (1972), McTaggart-Cowan and List (1975), and Bradley and Stow (1978). The results of

* Coastal Oceanography Division, Bedford Institute of Oceanography, Box 1006, Dartmouth, N.S., Canada B2Y 4A2.

** Atmospheric Environment Service, 4905 Dufferin Street, Downsview, Ontario, Canada M3H 5T4.

the first two have been incorporated into numerical models (Brazier-Smith et al., 1973; List and Gillespie, 1976). Low and List (1982, hereafter LL) extended the results of McTaggart-Cowan and List, producing the most complete parameterization currently available. The parameterizations of the List series of experiments have increased in complication and the current work examines the implications of the improved version. Other studies with LL parameterization have been carried out in the past two years by Donaldson (1984) for box and time dependent shaft models, and by Valdez and Young (1985, hereafter VY) and Brown (1986) for box models. We will use the present results to complement some aspects of collisional equilibrium already noted for box models and add new insight on drop evolution as it occurs in 1-dimensional rainshafts.

Unfortunately, several misprints occurred in the formulas as they appear in LL; the plotted diagrams, however, are correct. Since several workers have requested it, we include a list of corrections in appendix A. Given the extent and complexities of the parameterization, we do not repeat the whole set of equations and refer the reader to the original work of LL. It should be noted that these corrections were used by VY and Brown (1986).

2. Equations

In this section the equations describing collisional drop interactions will be given and converted to a form amenable to numerical solution. While much of this overlaps parts of previously published work, we wish to define our terms and develop an important new analytical result. To keep the equations as simple as possible, the drop spectra will be described in terms of drop mass, rather than drop diameter, as is more commonly done. The number of drops per unit volume, N, with masses between m and $m + dm$ will be given by

$$N = n(m)dm \tag{1}$$

where $n(m)$ will be referred to as the drop spectrum. It is convenient to represent the spectra on a logarithmic coordinate. In this case, N will be given by

$$N = a(l)dl \tag{2}$$

where l is the natural logarithm of the diameter:

$$l = \ln(D) \tag{3}$$

In addition to these number spectra, mass density (liquid water content) distributions can be defined as well. If M is the water mass per unit volume contained in drops with sizes between l and $l + dl$, it will be given by

$$M = g(l)dl. \tag{4}$$

To describe the evolution of a drop population through collisional interactions two things must be known. It must be known first how often drops of given sizes will collide, and, second, what the detailed outcome of each collision is.

The collision rate is easily described formally, although there is some problem on what constitutes a collision. Thus, some care must be taken to insure consistency when mixing results from different authors. Some include bounce-off in the collision category, but, for the purpose of this paper, such interactions will not be considered since they produce no change in the drop spectrum. The rate, A, at which collisions occur between drops of masses x and y (per unit time and volume) is given by

$$A = C(x, y)n(x)n(y)dydx \tag{5}$$

where $C(x, y)$ will be called the fractional interaction rate and is given by

$$C(x, y) = 0.25\pi(D_x + D_y)^2|\Delta v|E_{\text{coll}} \tag{6}$$

where $|\Delta v|$ is the difference in the terminal velocities, D_x and D_y are the drop diameters, and E_{coll} is the collision efficiency.

The description of the results of a collision is more complicated. A collision can produce either a coalescence or a breakup. A collisional breakup shall be defined to have occurred when, immediately after a collision, a temporarily combined pair of drops breaks into two or more drops. Low and List describe the results in terms of a fragment distribution $P(m; x, y)$ which gives the number of drops S produced per collision, having masses between m and $m + dm$, due to a collision between drops of masses x and y:

$$S = P(m; x, y)dm. \tag{7}$$

The fragment distribution is symmetric in terms of x and y, and is zero whenever $m > x + y$.

The number of drops produced with drop mass m will be the product of the fragment distribution and the interaction rate. If one considers all possible interactions then

$$\frac{dn(m)}{dt} = \int_{m/2}^{\infty}\int_{m-x}^{x} P(m; x, y)E_{\text{bu}}C(x, y)n(x)n(y)dydx \tag{8}$$

where E_{bu} is the breakup efficiency and the lower limit of the inner integral is zero when $m - x < 0$. The lower x limit indicates that the larger interacting drop must be at least half of m. The smaller drop can be no larger than x and must, in combination with x, provide at least enough mass to produce m. Here dn/dt is the total derivative given by

$$\frac{dn(m, z, t)}{dt} = \frac{\partial n}{\partial t} + \frac{\partial}{\partial z}(v_T n) \tag{9}$$

where v_T is the terminal velocity of an m-drop. Each collision will remove the initial (interacting) drops from the spectrum. This removal can be incorporated into

the interaction integral by means of Dirac delta functions, giving

$$\frac{dn(m)}{dt} = \int_{m/2}^{\infty}\int_{m-x}^{x} [P(m;x,y) - \delta(m-x) - \delta(m-y)]E_{bu}C(x,y)n(x)n(y)dydx. \quad (10)$$

The effects of coalescence can be included in the framework by means of a Dirac delta function at the mass of the coalesced drop ($m = x + y$).

The equation (with coalescence included) can be formally simplified to

$$\frac{dn(m)}{dt} = \int_{m/2}^{\infty}\int_{m-x}^{x} K(m;x,y)n(x)n(y)dydx \quad (11)$$

where $K(m; x, y)$ contains the description of the results of collisions. For simplicity, $K(m; x, y)$ will be referred to as the "kernel". It is given by

$$K(m;x,y) = [E_{bu}P(m;x,y) + E_{coal}\delta(x+y-m) - \delta(m-x) - \delta(m-y)]C(x,y). \quad (12)$$

Equation 11 is of a simple form, but the complication of the kernel prevents analytic solution. Solution of the full equation requires the development of a numerical solution technique. An important result, that has not been previously noted, can be drawn from equation 11 regarding collisional equilibria. At equilibrium the spectrum has adjusted itself so that

$$\int_{m/2}^{\infty}\int_{m-x}^{x} K(m;x,y)n(x)n(y)dydx = 0. \quad (13)$$

If $n'(m)$ is a solution of Eq. 13 for a given liquid water content, it can be seen that any multiple of $n'(m)$ is also a solution. Thus a family of equilibrium distributions can be described by means of a shape function that gives the variation in terms of drop size and a scaling function that describes the variation in terms of the liquid water content. For comparison to the standard form of the Marshall-Palmer equation (Marshall and Palmer, 1948), the scaling factor can be expressed in terms of the rainfall rate, R, and the shape function in terms of the diameter, D. With these variables, it can be easily shown that a family of equilibrium curves is defined by

$$f(D,R) = R\psi(D) \quad (14)$$

where $\psi(D)$ is the shape function. This is true, regardless of the physics of the collisional process, and substantiates VY's speculation that the intercept N_0 of an exponential distribution is generally proportional to R (or LWC) at equilibrium, i.e.

$$f(D,R) = cRe^{-\lambda D} \quad (15)$$

but obviously negates their speculation about deviation from proportionality.

Until the details of the kernel $K(m; x, y)$ are known, nothing can be said about the shape of the equilibrium curves, nor can one say whether there is more than one family of equilibrium curves. (The numerical experiments of both VY and ourselves indicate that there is only one such family for the Low/List kernel.) The standard Marshall–Palmer equation, describing observed spectra in terms of R and D, averaged over many rain events, but within a limited specified rainfall range, is very different from the form given by Eq. 14. On a semilog display the Marshall–Palmer equation shows spectra for different rainfall rates radiating out from a single point once the constants are chosen, whereas Eq. 14 predicts parallel curves. This latter is essentially what is seen in VY, Brown (1986), and in the present paper, although there are some deviations which are presumably due to true equilibrium not having been reached. In particular, Table 2 of VY would seem to indicate that their "equilibrium spectra" were not in fact completely at equilibrium and their discussion of the table may be misleading. Gillespie and List (1978) also arrived at essentially parallel equilibrium distributions, which they approximated by Marshall–Palmer type distributions. A family of exponential equilibrium distributions is basically possible, as these authors showed, if N_0 were a function of the rainfall rate and the exponent were independent of it.

To solve Eq. 11, the technique of Gelbard and Seinfeld (1978) was extended to include breakup. The technique is basically the same as those used by Gillespie and List (1978), Brown (1986) and others, as discussed by Donaldson (1984). Since the sensitivity of the model to some underlying parameters is examined, a brief description is given here. For the numerical scheme the continuous variable of drop mass is divided into a series of 'bins". The exponentially expanding coordinate of Berry and Reinhardt (1974) was used to define the divisions between bins. For the numerical experiments described below, the drop mass at the dividing points doubled every two bins. Within each bin an integral quantity of the spectrum was used to represent the spectrum. This quantity, Q, could be any integral over a bin of any property $\phi(x)$ of the drops,

$$Q = \int_{m_k}^{m_{k+1}} \phi(x)n(x)dx, \quad (16)$$

but in practice, Q was chosen to be the mass within each bin. Thus Q for bin k was defined by

$$Q_k = \int_{m_k}^{m_{k+1}} xn(x)dx \quad (17)$$

where the ends of bin k are denoted by m_k and m_{k+1}.

To convert Eq. 11 into an algebraic form amenable to computer solution, its integrals are subdivided into a series of integrals, each of which is over a single bin. Since the spectrum $n(x)$ is not known within the bins, it must be reconstructed, using the Q_k. This is done

by means of an assumed shape function $V_k(x)$ within each bin:

$$n_k(x) = Q_k V_k(x). \tag{18}$$

With these changes, Eq. 11 becomes an equation for the evolution of the Q_k:

$$\frac{dQ_k}{dt} = \sum_{i=1}^{n-1} \sum_{j=1}^{i} X_{ijk} Q_i Q_j \tag{19}$$

where $n-1$ is the number of bins into which the drop mass range has been divided, and where X_{ijk} is given by

$$X_{ijk} = \int_{m_i}^{m_{i+1}} V_i(x) \int_{m_j}^{m_{j+1}} V_j(y) \int_{m_k}^{m_{k+1}} wK(w;x,y)dwdydx \tag{20}$$

if $i \neq j$ and half this value if $i = j$.

The matrix equation (19) has several advantages. The complicated kernel has been converted into a matrix which need only be evaluated initially, since it will remain unchanged for all calculations using the same division into bins. This is a significant computational saving with a kernel as complicated as that of Low and List. Further, the equation as developed conserves the water mass content in the spectrum, provided that the original $P(m; x, y)$ conserves mass. The parameterization as described in LL does not conserve mass exactly, so minor corrections were necessary. In some instances, away from observed data points, the LL parameterization can produce mass increases from breakup by a few percent. In these cases the entire fragment distribution $P(m; x, y)$ was scaled down to match the mass of the initial drops before collision. In contrast to other corrections considered, this roughly preserves predicted drop numbers, which was one of the measured parameters in the experiment. Since the correction was necessary for conditions where there was no observational data, a simple correction seemed best. (The LL parameterization gives fragment number distributions for any size combination of colliding drops in the form of a four-dimensional surface in phase space. To build in exact mass conservation would be a major undertaking.) In addition to mass conservation, caution was necessary to correctly integrate the fragment distribution near the initial drop sizes, since the peaks can be very narrow. Brown (personal communication, 1986) also found that great care was necessary in the numerical integrations. Despite these problems, the difficulties are not as severe as implied by VY.

Equation (19) is similar to Gillespie and List's (1978) extension of the technique of Danielsen et al. (1972) and is analytically identical if the appropriate shape function is chosen. On the other hand, implicit differences in the technique yield significant advantages, since the use of several separate integral terms leads to unnecessary rounding errors when differences are taken between large numbers. In the current scheme the differences are done carefully in the calculation of X_{ijk}, before the summations are done. One disadvantage of this technique is that it does not allow for a study of the separate microphysical processes of drop creation, destruction, and modification. It may be that VY's technique for following drop identity in a Markov model is better suited to that type of analysis, but the precise technique for converting the fragment distribution into transition probabilities (especially those involving the additional nonphysical bin) is not clear to us. VY also do not explain the technique for handling statistical nonstationarity, when the drop spectrum is not at equilibrium. As a result, we do not wish to speculate too far on the relative merits of the two techniques.

An investigation of the effects of choosing different shape functions was made. Since Q_k and X_{ijk} are essentially weighted averages over the bins (with the weighting determined by the shape functions), changes in the shape function could influence the accuracy of the model, but would not be expected to do so if the bins were sufficiently narrow. The shape function was originally introduced with a view to enabling relatively few bins to give a good estimate of the spectrum, by using shapes that were close to those displayed by the spectrum. As will be seen however, the spectrum shape evolves widely enough that no set of fixed shapes can give a good approximation to the spectrum across wide mass bins. It is thus necessary to use narrow bins (here, mass doubling every two bins, with $\sim$53–60 μm for bin 1), and thus the type of averaging implied by the shape functions makes little difference to the values of either Q_k or X_{ijk}. Three types of shape functions were tested: $V(x)$ constant (as in Gillespie and List, 1978), $V(x)$ proportional to $x^{-2/3}$ (e.g., $f(D)$ constant), and $V(x)$ proportional to $e^{-\lambda x}$ (inspired by a Marshall–Palmer type distribution). The maximum variation in any value of X_{ijk} or the initial values of Q_k was 3%. Given this insensitivity, $V(x)$ was chosen to be constant in each interval, since this was simplest.

The model performance was tested using artificial analytic kernels and confirmed the accuracy of the evaluation of the integrals of the right hand side of Eq. (11). The parameterization of Brazier-Smith et al. (1972) was also run, reproducing the results of Brazier-Smith et al. (1973), except for slight differences which are attributed to small differences in the handling of drops which grow to sizes outside the modeled drop size range.

3. Evolution towards equilibrium spectra in box models

To examine the evolution toward equilibrium distributions of the LL parameterization, the numerical scheme [Eq. (19)] was incorporated into a box model. The advective term in Eq. (9) was set to zero and Eq. (11) was solved as a solely time-dependent problem.

This is equivalent to assuming that the spectrum is evolving identically at all levels in an atmosphere of constant air density.

To obtain the equilibrium distributions for collisional processes, a numerical integration was done with time steps of one second, for two hours of simulated time and for various rainfall rates. After this period the initial spectra, which were Marshall–Palmer distributions, had evolved into those in Fig. 1. Although a two hour period is not sufficiently long for the lowest rainfall rates to have reached equilibrium, it can be seen that the spectra shown are essentially multiples of one another, in accordance with Eq. (14). The equilibrium shape function is trimodal, with the largest number of drops concentrated around at a diameter of 268 μm, and the majority of the mass in a peak at 1760 μm. A third peak is situated between the other two, at a diameter of 790 μm. Note that these numbers relate

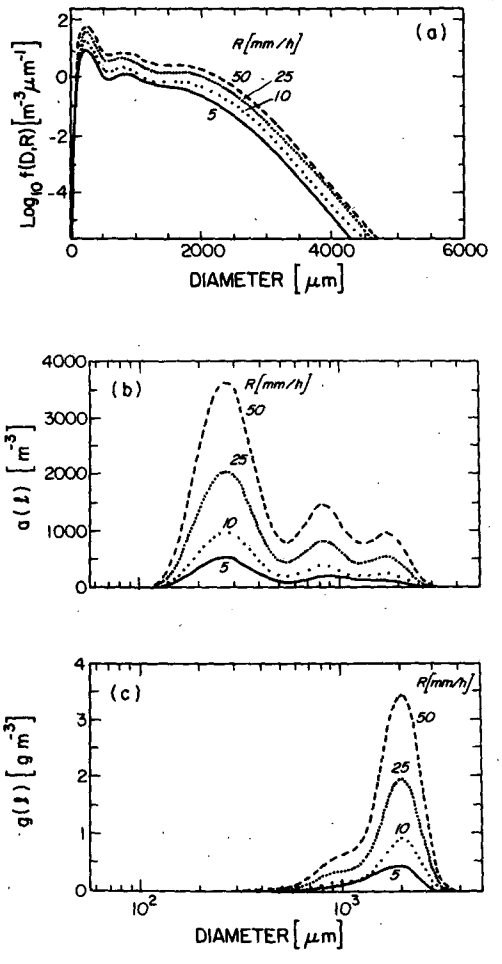

FIG. 1. Equilibrium distributions as evolved in box model after 2 h from Marshall–Palmer distributions with nominal rainfall rates of 5, 10, 25 and 50 mm h^{-1}, in different coordinate systems; number distributions in terms of (a) diameter, and (b) l[=ln(D)], (c) represents mass distributions in terms of l.

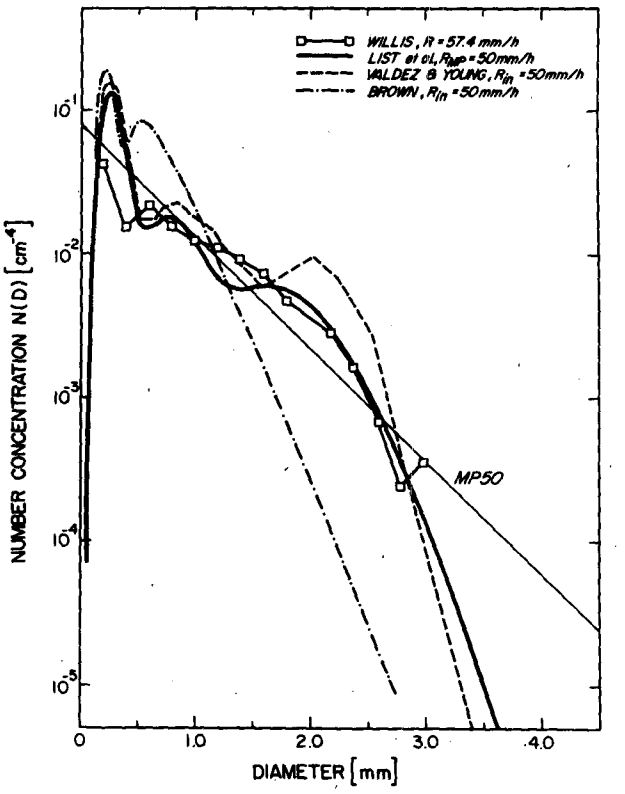

FIG. 2. Drop number concentration $N(D)$ for a Marshall–Palmer distribution MP50 for a rainfall rate R = 50 mm h^{-1}, equilibrium spectra as calculated for box models by present authors (solid line), and as extrapolated from data by Valdez and Young (1985) and Brown (1986), for some R. Data points by Willis (1984) indicate measurements in a hurricane.

to $a(l)$. This agrees well with the results shown by VY who covered rainfall rates 41 $\leq R \leq$ 207.5 mm h^{-1} and to a lesser degree with Brown (1986), who does not show a peak at 1760 μm. The results of the different authors are displaced in Fig. 2. Those for the peaks of ln$f(D)$ are slightly different, while the peak at smallest diameters is hardly reflected in $g(l)$. [It shoud be noted that ratios between equilibrium spectra in Fig. 1 are not the same as those of the nominal rainfall rates of the initial Marshall–Palmer distributions. Rather the ratios reflect the rainfall rates at equilibrium or, equivalently, the LWC of the initial spectra (box models conserve LWC).]

Distributions of radar reflectivities were also calculated. However, the heavy sixth-power weighting of diameter resulted in a spectrum that was based nearly entirely on the largest two or three bins, thus containing no information about two of the three number concentration peaks. Since the largest bins are the widest ones and those most strongly affected by the boundary conditions at the largest drop size, the calculated radar reflectivities were considered questionable due to lack of information.

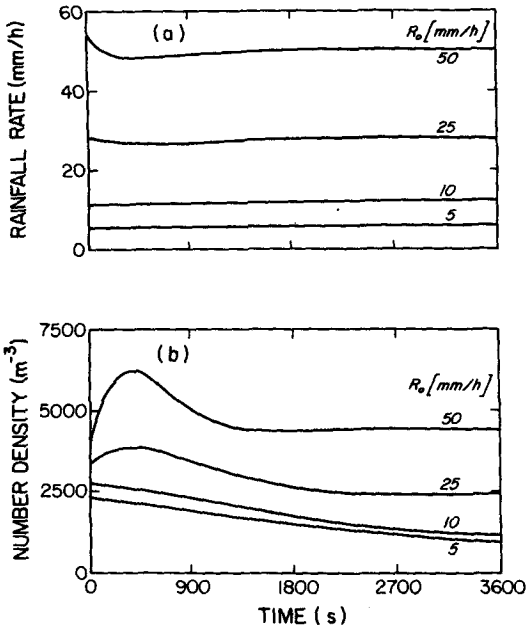

FIG. 3. Time evolution in box model of (a) rainfall rates and (b) of number density, away from Marshall–Palmer distributions, using the Low–List parameterization. Initially the nominal rainfall rates R_0 are 5, 10, 25 and 50 mm h^{-1}.

The collisional equilibrium is dynamic, in the sense that there is no cessation of collisional processes. Water is being exchanged between the various drop sizes so that each drop size loses as much as it gains. The interconnections between sizes are complicated, but an approximate interpretation of the equilibrium shape may be given. Breakups of larger drops produce the peak of such drops in the vicinity of 264 μm diameter. (The LL scheme produces few drops at sizes smaller than 140 μm and coalescence has removed any small drops initially present.) The smallest drops become sufficiently numerous so that they are collected by larger drops at the same rate at which they are created. For large drops and the most common breakup type by filament, the LL breakup parameterization predicts that collisions will usually produce two drops that are slightly smaller than those entering the collision. This leads to the concentration of mass in drops in the vicinity of 1760 μm. Drops have grown to the large sizes by coalescence and partial coalescence, but are effectively restricted from further growth. The origin of the intermediate peak is unclear, but, since it does not appear until after the small peak develops, it seems likely that it requires the presence of a substantial number of small drops. This intermediate peak appears near the dividing point between what VY call the "landed" and "nomadic" conceptual models, and the situation is expected to be complicated. Using their special technique, VY give a more physical interpretation that agrees with this analysis of equilibrium fluxes.

The sharpness of the peaks of the equilibrium curve was observed to depend on the widths of the bins of the numerical model. With mass doubling every bin, the center peak was less distinct and merged with the peak at small drop radius, but this had no effect on the trimodal distribution. Experiments with higher resolution were prohibited by computing restrictions.

The possibility of finding collisional equilibria in nature depends on the time available for them to form. For the box model, Fig. 3 shows the evolution of the rainfall rate and the total drop number density away from initial Marshall–Palmer distributions with nominal rainfall rates of 5, 10, 25 and 50 mm h^{-1}. From these curves it can be seen that high rainfall rates (50 mm h^{-1} and above) reach equilibrium in times under ½–¾ hour. On the other hand, the drop populations which initially had lower rainfall rates (under 10 mm h^{-1}) show no indication of approaching equilibrium after one hour, although an extension of the integration to two hours shows the 10 mm h^{-1} case approaching equilibrium. The times to reach equilibrium show the expected qualitative dependence on liquid water content.

Similar time integrations were done, starting with other (non-Marshall–Palmer) distributions. The equilibrium shapes were the same and the time scales for evolution were approximately the same for equivalent liquid water contents, showing only slight dependence on the initial spectrum shape. Figure 4 shows the evolution of the number density N and the rainfall rate R

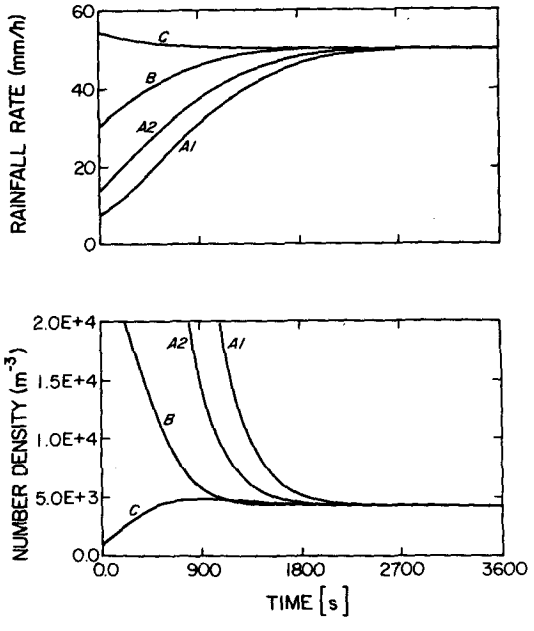

FIG. 4. Time evolution in box model away from Gaussian distributions of (a) rainfall rates and (b) number density as characterized in Table 1. All distributions have liquid water contents equal to that of the Marshall–Palmer distribution for a rainfall rate of 50 mm h^{-1}.

TABLE 1. Characteristics of Gaussian distributions.

Run	Mode	σ
A1	$D_0 = 172\ \mu$	0.3
A2	$D_0 = 170\ \mu$	0.5
B	$D_0 = 400\ \mu$	0.5
C	$D_0 = 1500\ \mu$	0.3

for four spectra that were initially Gaussian in the coordinate l, with liquid water contents equivalent to that of a Marshall–Palmer distribution with a rainfall rate $R = 50$ mm h^{-1}. The Gaussians are specified by the equation

$$a(l) = A \exp\{[(l - \ln(D_0))/\sigma]^2\} \qquad (21)$$

and the parameters chosen are specified in Table 1.

Again, the times to reach equilibrium are long, and the corresponding heights of fall are in excess of several kilometers. Nonetheless, a knowledge of the equilibrium spectrum shape is useful, since it is toward this that all spectra tend to evolve.

Figure 5 shows three stages in the evolution away from Marshall–Palmer distributions with nominal rainfall rates of 5 and 50 mm h^{-1}. The plots show scaled distributions $a(l)$ (solid) and $g(l)$ (dotted) in a manner

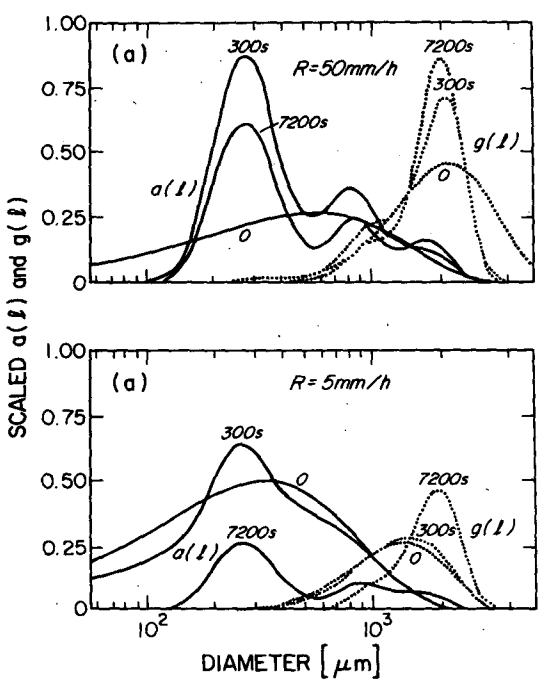

FIG. 5. Stages of evolution in box model of the number (a) and mass (b) distributions. Times are 0, 300 and 7200 s. Solid lines are $a(l)$ and dotted lines are $g(l)$. The spectra have been scaled for display in individual boxes.

Top: $R = 50$ mm h^{-1} $a(l)/4$, $g(l)/6000$

Bottom: $R = 5$ mm h^{-1} $a(l)/1$, $g(l)/2000$

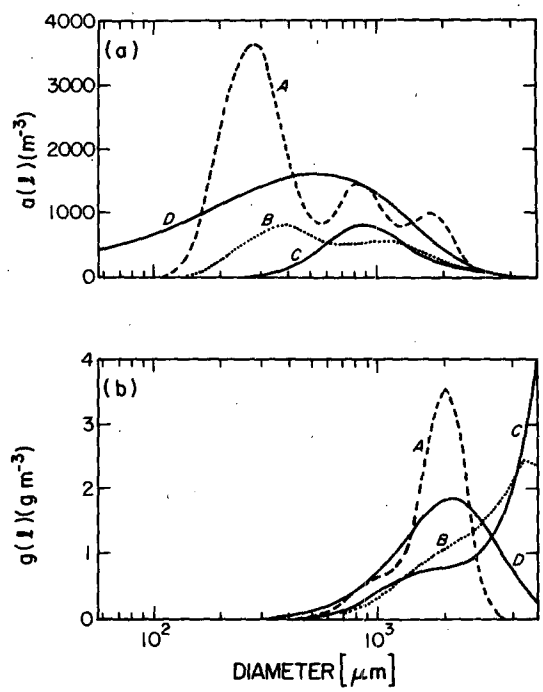

FIG. 6. Spectra in box model after 2 hours for (a) number and (b) mass concentration. The initial spectrum (D) was the Marshall–Palmer distribution for 50 mm h^{-1}. Three kernels are compared: (A) Low/List (B) Brazier-Smith et al., and (C) Hall.

which allows easy comparison of the development of the large and small peaks. Although the 5 mm h^{-1} case requires in excess of two hours to reach equilibrium, the peak at 264 μm is evident within five minutes. There is also indication after five minutes of the movement of mass toward the peak at 1760 μm. For the 50 mm h^{-1} case all the features of the equilibrium shape are present within five minutes.

For comparison to results obtained with other collisional parameterizations, the box model was run with two other schemes. The first uses the results of Brazier-Smith et al. (1972), and the second is a coalescence parameterization compiled by Hall (1981). Neither of these schemes limits drop growth so a condition must be imposed at the upper boundary of the largest drop bin. Hall used the scheme proposed by Danielsen et al. (1972), and it is also adopted here. The scheme redistributes drops growing to sizes outside the modelled range into a Gaussian centred at 1300 μm. Figure 6 shows results for the three parameterizations after 2 hours. It can be seen that the two simple parameterizations have not limited the movement of water to large drop sizes and the mass has effectively pushed up against the largest drop size available in the model. For the coalescence scheme the number distribution shows a peak due to redistribution of mass from the upper boundary. The Brazier-Smith results are more complex, with a peak in the number distribution near 400 μm reflecting the breakup products. Details of the evo-

lutions can be found in Donaldson (1984), but it can be seen that the increased detail of the LL parameterization has produced new detail in the spectrum and a limitation on drop growth.

Finally, as a side note to the box model, we wish to briefly mention results obtained with evaporation. The model was subsaturated, with the evaporation (diffusion) equations included in the microphysics, but the lowest relative humidity was 95% because of numerical stability limitations. The results showed that although the evaporative process removes small drops preferentially, the collisional processes mix water between sizes and tend to counter the selective removal of water from small drops by spreading the loss across the spectrum. Thus, for large rainfall rates, the spectrum shapes were virtually the same as for the saturated cases, except that the LWC continually decreased due to the removal of water by evaporation.

4. A time-dependent shaft model

To examine interactions between spatial and temporal evolution, collisions were studied in a time-dependent shaft of constant air density. Equation (9) was solved using the numerical scheme of Eq. (19). This models a one-dimensional rainshaft that is evolving in time in response to a spectra imposed at the top. Since evaporative effects are not considered here, the shaft was regarded as being saturated with respect to water vapour. It is assumed that there are no vertical motions and no dependence of the drops' terminal velocities with height. The latter simplification is justified by the fact that dependence of the kernel $K(m; x, y)$ is not known, although List and Fung (1982) have shown that collisional processes do depend somewhat on height. The effect of the inclusion of the vertical variation in air density and thus in terminal velocity would be to increase the number density by a few percent near the ground, with a corresponding increase in the collision rate. To complete the specification of the spectral evolution it is necessary to provide a spectrum throughout the shaft at $t = 0$ and to specify the spectrum at the model top at all times.

While matching the CFL numerical criterion for large drops, ordinary finite difference techniques on a fixed grid would produce a very high numerical diffusion for the smallest droplets. For the drop sizes considered, the terminal velocity varies over two orders of magnitude, making it impossible to tune the space and time increments to produce acceptable diffusion rates in all bins. (We do not believe that this numerical diffusion would model real turbulent diffusion in any serendipitous way.) Tests of a prototype fixed grid model with no microphysics showed substantial number of droplets falling 2 km in times which should only allow falls of 100 m. To avoid this problem a "conveyor belt" model was adopted. The number distribution, $f(D, z)$, was first divided into diameter bins and then similarly divided into vertical sections. With each time step each column of vertical bins was lowered according to the average terminal velocity of the drops in that diameter bin. For the calculation of the collisional evolution, the vertical was divided into levels and all vertical sections and bins at that level were averaged to produce a drop spectrum. The technique reproduces exactly the spectrum of drops falling in the absence of microphysics. It was initially suspected that this might combine with the microphysics to produce unreasonable vertical cross diffusion of the small drop population, but that was not the case. Steady state spectra were correctly reproduced when the model was run sufficiently long. As VY point out, birth/destruction events dominate the small drop population and those effects overwhelm errors in to the vertical representation. For large drops the representational problem is negligible, due to the higher vertical velocities. The advantage of this technique is that it allowed a vertical subresolution on the order of 10 m while restricting the expensive calculation of breakup to intervals of the order of 100 m.

The simplest case is that of a shaft that is initially devoid of drops but which has a constant drop spectrum specified at the top and evolves with time. Figure 7 shows such a case. The contours are isolines of the number spectrum $a(l)$ and of the mass density $g(l)$ after 600 seconds. A Marshall–Palmer spectrum with a nominal rainfall rate of 50 mm h^{-1} was imposed at the shaft top, starting at $t = 0$. The heavy solid line represents the position of drops which were at the shaft top at $t = 0$, were they to fall without interaction (the

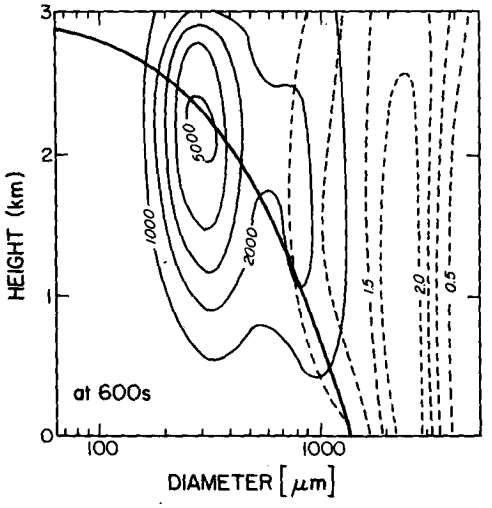

FIG. 7. Time dependent *rainshaft* after 600 s. At $t = 0$ the rainshaft was empty and rain in Marshall–Palmer form of a nominal rate of 50 mm h^{-1} was introduced. The thick line represents the distance fallen by drops of different radii introduced at time zero. Solid contours (interval 1000 m^{-3}) are for the number distribution $a(l)$, while the dashed contours (interval 0.5 g m^{-3}) are for the mass distribution $g(l)$.

"fall line"). In the case shown, a great many drops appear below the fall line, indicating that these drops were created close to the level of occurrence, rather than having fallen from the top. Drops with diameters near 200 μm are being created two kilometers below the level to which they could have fallen. This new population of small drops is created by breakups of the large drops. An observer at the ground would initially see the arrival of the very largest drops. As more drops appear the large drop spectrum widens and collisions become more frequent. Shortly after drops with diameters near 1760 μm appear there is a rapid widening of the spectrum, caused by collisional breakup. This evolution is very similar to that typically observed during the onset of a rain shower. At very large times the shaft becomes steady state, with a progressive evolution towards the equilibrium shape as the ground is approached. For high rainfall rates ($R \geq 50$ mm h^{-1}) the spectrum at the ground has essentially acquired the equilibrium shape after 3 km of fall.

To examine interactions between a series of pulses of rain, a sinusoidally varying spectrum was specified at the shaft top by multiplying a Marshall–Palmer distribution by 0.5 (1 + cosωt). Thus the spectrum is of fixed shape, with an oscillating number concentration. Figure 8 shows results from the case where the spectrum at the top varied with a period of 300 seconds, peaking in a Marshall–Palmer distribution with a nominal rainfall rate of 50 mm h^{-1}. (This period was selected as typical of variations in observed rain pulses.) The figure shows the shaft at times half a period apart, after a period of time long enough that the effect of the initial population has vanished. A comparison of the shaft at times displayed shows that the large drop population is propagating downward virtually unchanged, although there is a slight narrowing by the collisional processes. At a given level the large drop population varies in rough accordance to the variation at the shaft top. The small drop population, on the other hand, is very nearly steady. Figure 9 shows the spectra at the ground at the times shown in Fig. 8.

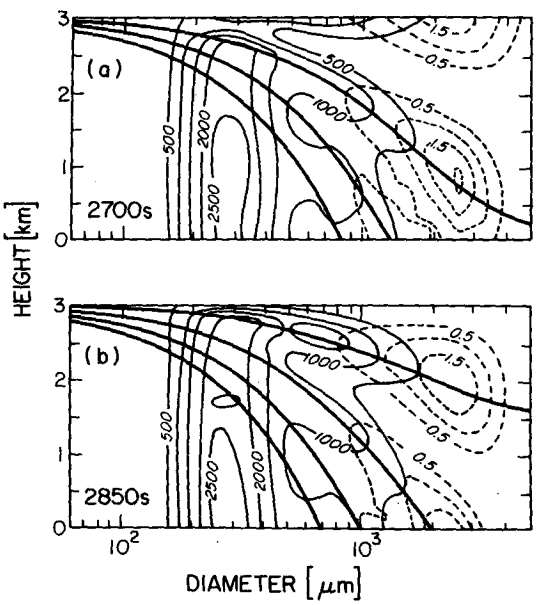

FIG. 8. Time dependent *rainshaft* after (a) 2700 s and (b) 2850 s. An oscillating Marshall–Palmer distribution (period 300 s) is being introduced at the shaft top. The thick lines represent the distances fallen by drops introduced when the rainfall peaked. Solid contours (interval 500 m^{-3}) are for the number distribution $a(l)$, while the dashed contours (interval 0.5 g m^{-3}) are for the mass distribution $g(l)$.

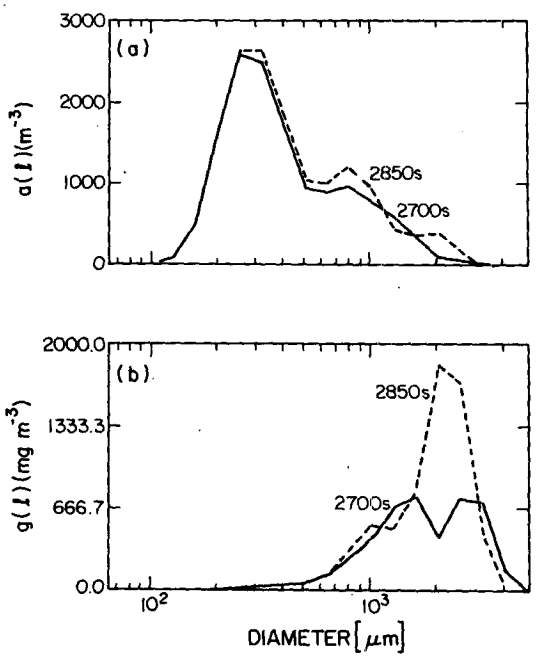

FIG. 9. Spectra at the ground. The spectra are from the rainshaft simulation shown in Fig. 8. The solid lines are spectra after 2700 s and the dashed lines spectra after 2850 s. These spectra are half a period of the rainfall rate pulsation apart.

5. Conclusions and discussion

Equation (14) predicts equilibria of raindrop size distributions, with families of solutions wherein the equilibria for different rainfall rate are multiples of one another. The equilibrium shape is independent of the origin of the rain and the early drop size distribution. This was also shown in box models and in one-dimensional steady-state and time dependent models of rainshafts. Examination of earlier numerical results, such as those of Brazier Smith et al. (1973) and Gillespie and List (1978) show equilibria at different rainfall rates that have a multiplicative relationship.

A family of curves was found for the collisional breakup parameterization of Low and List (1982). The spectra are trimodal and contain peaks near drop diameters of 268, 790 and 1760 μm. They closely resem-

ble those of VY and somewhat those of Brown (1986). However, Brown has no peak for large drops. The equilibrium distributions have more structure than those reported by List and Gillespie (1976) because the Low and List (1982) collision/breakup data have a higher resolution than those by McTaggart-Cowan and List (1975) which formed the basis for List and Gillespie. Thus the parameterization by LL more accurately reflects the improved laboratory results. The equilibrium spectra are the same for the box model and the one-dimensional rainshaft model.

Equilibrium distributions take time to evolve, particularly at low rainfall rates (up to 2 h and more for rainfall rates of less than 10 mm h^{-1}), but their main features become obvious within 5–10 minutes. The same equilibria are obtained for original spectra described by Marshall–Palmer or four different Gaussian distributions. In natural spectra of steady rain, deviations from equilibrium are indicative of not yet developed equilibria, the evolution of rain with height and possibly also its origin, be it in the form of a "warm rain" or "cold rain".

With the limited range of testing it was found that, while evaporation prefers removal of small drops, the collisional processes rapidly mix such losses across the whole spectrum. This results in a reduction of the LWC by evaporative effects, but without a change in shape of the drop size distribution. This could be of importance in the numerical modeling of evaporative effects related to rain in the subcloud layer.

The time dependent shaft model gives a good explanation why, as often observed, rain commences with the arrival of large drops, which somewhat later give way to a mix of smaller and larger drops. The same model also shows that the small drops at the ground do not reflect a part of the spectrum at the cloud base. They are results of the collision/breakup process involving the larger drops during fall. This is basically the reason for the existence of equilibrium spectra. The numerical experiment with a pulsating rainfall rate show that the pulsation is imposed on the concentration of the raindrops contained in the largest group (peak at diameters of 1760 μm). The rest of the number concentration spectrum is approximated by the equilibrium curve.

The work presented applies to warm clouds and to the warm or subfreezing levels (without ice) of clouds with ice particles in the subzero regions. However, the considerations can also be given to cold regions where warm rain may develop parallel to the ice particles, but with the additional interactions that occur between ice and water. This aspect will be important for a more elaborate treatment of the complexities of precipitation in the presence of graupel and hail.

The importance of this study lies in the possibility of field testing the conclusions in appropriate situations where equilibria might develop. This however, will require sophisticated measuring probes (PMS 2-DC and P type) at the ground and in subcloud aircraft because the size range needs to contain the three spectral modes. The lowest maxima may not be adequately resolved at the ground with a Joss distrometer, and radar would detect only the largest peak. The latter can easily be inferred from the mass spectrum in Fig. 1 which barely shows the existence of the 268 μm drops and relegates the 790 μm diameter drops into a shoulder of the larger group. There is an indication however, that these peaks have already been observed in nature within hurricane clouds in Florida (Willis, 1984, see Fig. 2).

The box and one-dimensional models used here do not contain height dependence of the microphysics. Basically the kernal X_{ijk} is height dependent due both to the effect of terminal velocity on the interaction rate $C(x, y)$ and to the effect of pressure on the outcome of the collisions themselves. However, the inclusion of such pressure effects would require computer storage of height dependent matrices X_{ijk}—a prohibitive undertaking at this moment. Considering the limited pressure dependency of breakup established by List and Fung (1982), this is also not an urgent problem as long as we concentrate on the spectra at the ground.

Acknowledgments. This work was carried out within a research program funded by the Natural Sciences and Engineering Research Council of Canada and the Canadian Atmospheric Environment Service. The authors are grateful for the help and advice they received from Drs. W. D. Hall and T. L. Clark of the National Center for Atmospheric Research, NCAR. Computer support was provided by the Atmospheric Physics Group, University of Toronto and NCAR in Boulder, Colorado which is funded by the National Science Foundation of the United States. One of the authors, N.R.D., would like to acknowledge personal support provided by the NSERC and NCAR.

APPENDIX

Corrections to Low–List Parameterization

Authors T. B. Low and R. List have noted typing errors in their article "Collision, Coalescence and Breakup of Raindrops Part II: Parameterization of Fragment Size Distributions" (*J. Atmos. Sci.*, 1982, **39**, 1607–1619). The equations (3.3), (3.5), (4.8), (4.27), (4.37) and (4.38) should read as follows:

$$\bar{F}_{f1} = [-2.25 \times 10^4 (D_L - 0.403)^2 - 37.9] D_S^{2.5} + 9.67(D_L + 0.170)^2 + 4.95 \quad (3.3)$$

$$D_{s0} = [(\bar{F}_{f1} - 2)/a'']^{1/b''} \quad (3.5)$$

$$H_{f1}^{-1} = \left(\frac{\pi}{2}\right)^{1/2} \left[1 + \mathrm{erf}\left(\frac{D_{\mathrm{coal}} - D_L}{\sqrt{2}\sigma_{f1}}\right)\right] \sigma_{f1} \quad (4.8)$$

$$D_{ss2} = 0.254 D_S^{0.413} \times \exp[(3.53 D_S - 2.51)(D_L - D_S)] \quad (4.27)$$

$$D_{dd2} = \exp[(-17.4D_S - 0.671)(D_L - D_S)]D_S \quad (4.37)$$

$$P_{d2}(D_{dd2}) = \frac{H_{d2}}{D_{dd2}} \exp(-0.5\sigma_{d2}^2)$$

$$= 8.84 D_S^{-2.52}(D_L - D_S)^{b*} \quad (4.38)$$

Equation (4.38) yields the probabilities in units of cm^{-1}.

Further it should be noted that the lower limit of CKE_0 is 0.893 μJ (p. 1612, second last paragraph) and that R_f and R_s for Table 2 (p. 1613) should have been corrected for $R_f + R_s > 1$ according to: $\alpha = (R_f + R_s)^{-1}$ with $R_f' = \alpha R_f$ and $R_s' = \alpha R_s$, where primes denote corrected values.

All diagrams and tables of this 1982 paper are based on the correct equations and require no changes.

REFERENCES

Bergeron, T., 1935: On the physics of clouds and precipitation. *Proc. Fifth Assembly UGGI,* Lisbon, **2,** p. 156.

Berry, E. X., and R. L. Reinhardt, 1974: An analysis of cloud drop growth by collection. Parts I and II. *J. Atmos. Sci.,* **31,** 1814–1831.

Bradley, S. G., and C. D. Stow, 1978: Collisions between liquid drops. *Phil. Trans. Roy. Soc. London,* **A287,** 635–678.

Brazier-Smith, P. R., S. G. Jennings and J. Latham, 1972: The interaction of falling water drops: Coalescence. *Proc. Roy. Soc. London,* **A326,** 393–408.

——, —— and ——, 1973: Raindrop interactions and rainfall rates within clouds. *Quart. J. Roy. Meteor. Soc.,* **99,** 260–272.

Brown, P. S., 1986: "Analysis of the Low and List drop-breakup formulation". *J. Climate Appl. Meteor.* **25,** 313–321.

Danielsen, E. F., R. Bleck and D. A. Morris, 1972: Hail growth by stochastic collection in a cumulus model. *J. Atmos. Sci.,* **29,** 135–155.

Donaldson, N. R., 1984: Raindrop evolution with collisional breakup: Theory and models. Ph.D. thesis, University of Toronto, Toronto, Ontario, Canada, pp. 181. [National Library of Canada, Ottawa, Canadian Thesis No. 66758.]

Gelbard, F., and J. H. Seinfeld, 1978: Numerical solution of the dynamic equation for particulate systems. *J. Comput. Phys.,* **28,** 357–375.

Gillespie, J. R., and R. List, 1978: Effects of collisions-induced breakup on drop size evolution in steady state rainshafts. *Pure Appl. Geophys.,* **117,** 599–626.

Hall, W. D., 1981: "A detailed microphysical model within a 2-dimensional framework". *J. Atmos. Sci.,* **37,** 2486–2507.

Langmuir, I., 1948: The production of rain by a chain reaction in cumulus clouds at temperatures above freezing. *J. Meteor.,* **5,** 175–192.

List, R., and C. Fung, 1982: Effect of pressure on the breakup of one pair of raindrops. *Atmos-Ocean,* **20,** 17–27.

——, and J. R. Gillespie, 1976: Evolution of raindrop spectra with collision-induced breakup. *J. Atmos. Sci.,* **33,** 2007–2013.

——, C. F. MacNeil and D. McTaggart-Cowan, 1970: "Laboratory investigations of temporary collisions of raindrops". *J. Geophys. Res.,* **75,** 7573–7580.

Low, T., and R. List, 1982: Collision, coalescence and breakup of raindrops. Parts I and II. *J. Atmos. Sci.,* **39,** 1591–1618.

Magarvey, R. H., and J. W. Geldart, 1962: Drop collisions under conditions of free fall. *J. Atmos. Sci.,* **19,** 107–113.

Marshall, J. S., and W. M. Palmer, 1948: The distribution of raindrops with size. *J. Meteor.,* **9,** 327–332.

McTaggart-Cowan, J. D., and R. List, 1975: Collision and breakup of water drops at terminal velocity. *J. Atmos. Sci.,* **32,** 1401–1411.

Middleton, W. K., 1966: *A History of the Theories of Rain and Other Forms of Precipitation.* F. Watts, 223 pp.

Pruppacher, H. R., and J. D. Klett, 1978: *"Microphysics of Clouds and Precipitation".* Reidel, 714 pp.

Reynolds, O., 1877: *Proc. Manchester Lit. and Phil. Soc.,* **16,** 23–33.

Valdez, M. P., and Young, K. C., 1985: "Number fluxes in equilibrium populations: A Markov chain analysis", *J. Atmos. Sci.,* **42,** 1024–1036.

Wegener, A., 1911: *"Thermodynamik der Atmosphäre".* J. A. Barth, Leipzig, 331 pp.

Willis, P. T., 1984: Functional fits of some observed drop size distributions and parameterization of rain, *J. Atmos. Sci.,* **41,** 1648–1661.